Review

Pathogenetic Role of Amyloid Precursor Protein in Alzheimer's Disease: The Internal Disintegration Hypothesis Revisited

Kazuaki Yoshikawa, ***M.D., Ph.D.***

Professor Emeritus
The University of Osaka

Summary

Alzheimer's disease is characterized by massive neuronal degeneration and extracellular amyloid deposition in the brain. Although there have been numerous studies exploring these pathological hallmarks, a causal relation between the two events remains elusive. The most prevailing idea is that the extracellular deposition of amyloid, which results from the polymerization of amyloid-β protein generated by abnormal processing of amyloid precursor protein (APP), leads to neuronal degeneration 'from outside' (the amyloid cascade hypothesis, 1992). The author of this review proposed an alternative hypothesis based on the analyses of APP-overexpressing cell models (the internal disintegration hypothesis, 1995). This hypothesis is that intraneuronal accumulations of APP and its amyloidogenic fragments generated in the lysosomes contribute primarily to neuronal death 'from inside', implying that the extracellular amyloid deposition is an accompanying event. Further studies have shown that caspase-3, a key apoptosis-executioner protease, is activated in APP-overexpressing degenerating neurons where the intracellular accumulation of APP leads to a sequential activation of the Ca^{2+}-activated protease calpain and caspase-3. Moreover, APP-induced apoptosis is likely to operate in nascent neurons during the early period of development. In this review, the author revisits the hypothesis and discusses that APP plays a neuroprotective role but induces neurodegeneration when its accumulation reaches a critical level to trigger the apoptotic pathway. This hypothesis has been corroborated by multiple lines of evidence in studies on mutant APP transgenic mice and neuropathological findings in Alzheimer's disease.

Key Words: APP, amyloid plaque, amyloidogenic fragment, neurodegeneration, apoptosis, caspase-3, calpain, lysosome, programmed cell death, Alzheimer's disease

Abbreviations: Aβ, amyloid β protein; AD, Alzheimer's disease; AP, amyloid plaque; APP, amyloid precursor protein; APP-C, APP carboxyl-terminal; APP-N, APP amino-terminal; Csp3, caspase-3; CTF, C-terminal fragment; DRG, dorsal root ganglion; EC, embryonal carcinoma; NFT, neurofibrillary tangle; NGF, nerve growth factor; RA, retinoic acid

I. Neuropathology of Alzheimer's disease

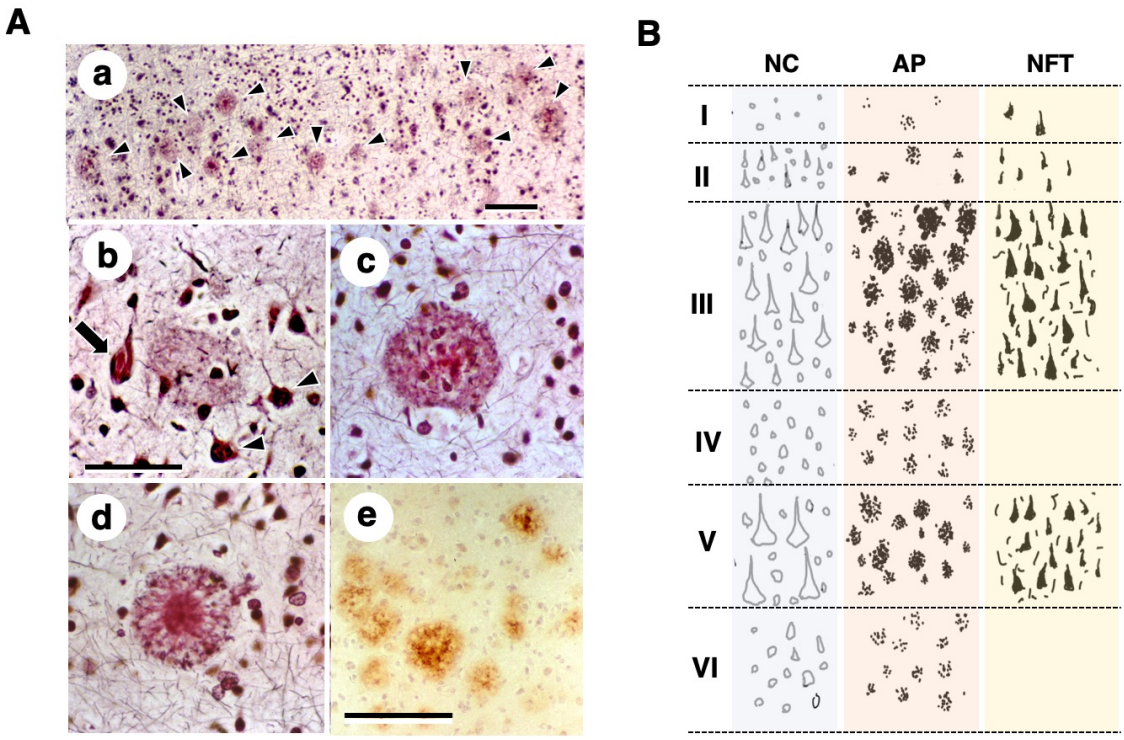

Figure 1. Neuropathology of Alzheimer's disease. ***A***: Amyloid plaque (AP) and neurofibrillary tangle (NFT). Brain sections of Alzheimer's disease (AD) cases were stained by Bielschowsky's silver staining. (***a***) Zonal distribution of AP (*arrowheads*). (***b***) AP and NFT (*arrowheads*, *arrow* points extracellular ghost tangle). (***c***) AP carrying amorphous amyloid deposits and dystrophic neurites. (***d***) AP with central amyloid core surrounded by dystrophic neurites. (***e***) Aβ-immunoreactive plaques. AD brain section was stained with antibody to Aβ. Scale bars: 100 μm (***a***, ***e***); 50 μm (in ***b*** for ***b***-***d***). Brain samples of AD cases were provided by Dr. Tsuyoshi Ishii. ***B***: Diagram of distribution patterns of AP and NFT in the neocortex affected by AD. Illustration based on neuropathological data stained with silver or thioflavin S (Braak et al., 1989; Arnold et al. 1991). AP and NFT are abundant in layers *III* and *V* where large pyramidal neurons reside. *NC*, neocortical layers *I*-*VI*.

Neuropathological hallmarks of Alzheimer's disease (AD) are massive neuronal death, amyloid plaques (APs) (also known as senile plaques or neuritic plaques) and neurofibrillary tangles (NFTs). APs are distributed in the extracellular area (Fig. 1Aa), whereas NFTs are formed inside neurons and persist in the extracellular space as ghost tangles after neuronal death (Fig. 1Ab). Because deposits of primitive APs are smaller, more diffuse than those of mature APs (Fig. 1Ab), it has been assumed that primitive APs with diffuse amyloid deposits develop for many years to mature plaques with dense amyloid deposits at the advanced stage of AD (Fig. 1Ac,d). Some of large plaques contain intensely Aβ-immunoreactive materials at the central area. Immunohistochemistry for amyloid β protein (Aβ), the principal component of amyloid fibrils, reveals the distribution of plaque-like deposits in various sizes in AD brain (Fig. 1Ae). Thus, the link between the formation of APs and neuronal loss in the brain has been central to AD pathogenesis. Densities of amyloid plaques and NFTs are significantly correlated (Braak et al., 1989; Arnold et al., 1991) (Fig. 1B).

APs and NFTs are predominantly distributed in the hippocampus and neocortical layers III and V, where large pyramidal neurons are abundant, suggesting that these pathological hallmarks correlate with the densities of neuron populations localized in the specific layers.

II. Aβ and its precursor protein APP

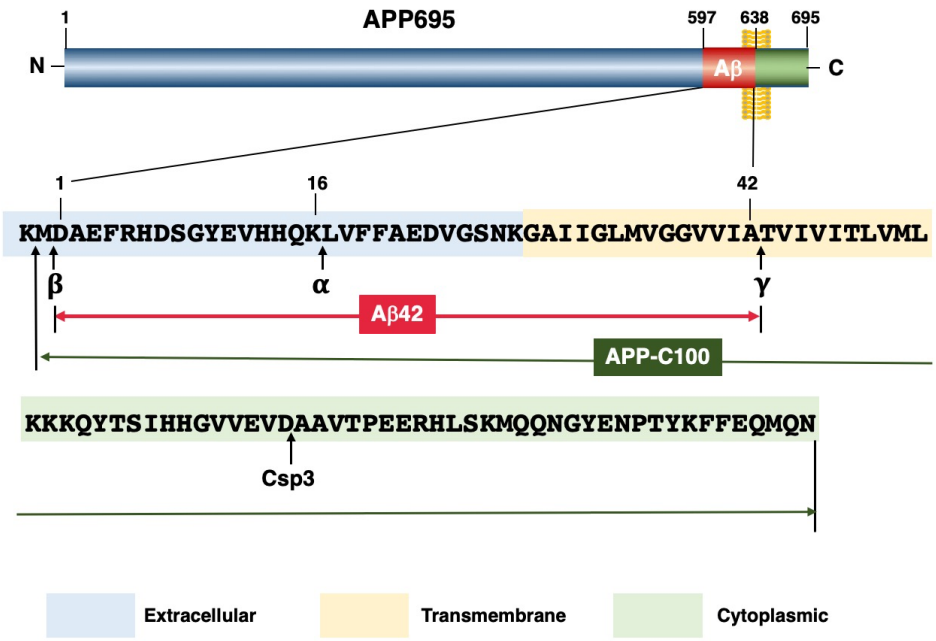

Figure 2. Aβ and its precursor protein APP. Only C-terminal sequences and positions of APP695 relevant to this review are shown. *Arrows* point to secretase cleavage sites (*α, β, γ*) and caspase-3 cleavage site (*Csp3*). Aβ42 (*Aβ42*) is generated from APP when cleaved at positions β and γ, but not at position α. Met (*M*) codon at the N-terminal of APP-C100 (*APP-C100*) is used as translation start codon. See text below for explanation.

Aβ was isolated from amyloid fibrils in cerebrovascular amyloidosis associated with AD (Glenner and Wong, 1984). Aβ is generated by the aberrant processing of a large transmembrane glycoprotein designated amyloid precursor protein (APP) (Kang et al., 1987). APP consists of large extracellular and small cytoplasmic domains (Fig. 2). The Aβ domain encompasses the junction of the extracellular and transmembrane domains. When APP is cleaved at the N-terminal (β cleavage) and C-terminal (γ cleavage) sites, Aβ42, a highly amyloidogenic peptide, is generated. Under physiological conditions, APP is cleaved at the middle site (α cleavage), which fails to generate Aβ42. Thus, cellular and molecular mechanisms whereby Aβ42 is generated from APP have been extensively studied to elucidate the pathogenesis of AD. Aβ42 polymerizes to form amyloid fibrils which are insoluble and resistant to degradation. Amyloid fibrils are characterized by helical structures consisting of β-pleated sheets as the secondary protein structure. Three species of APP (APP695, APP751, and APP770) mRNAs are generated through alternative splicing of a primary

transcript from the single APP gene located on chromosome 21, which is triplicated in Down syndrome. Among three APP species (APP695, APP751, and APP770), APP695, which lacks Kunitz-type protease inhibitor domains of APP751 and APP770, rapidly increases when postmitotic neurons are differentiated from P19 embryonal carcinoma (EC) cells, whereas APP751 and APP770 increase later in astrocytes and non-neuronal cells (Yoshikawa et al., 1990). Importantly, APP is highly concentrated in pyramidal neurons of the neocortex and hippocampus, where the densities of AP and NFT are high (Benowitz et al., 1989).

III. The amyloid cascade hypothesis

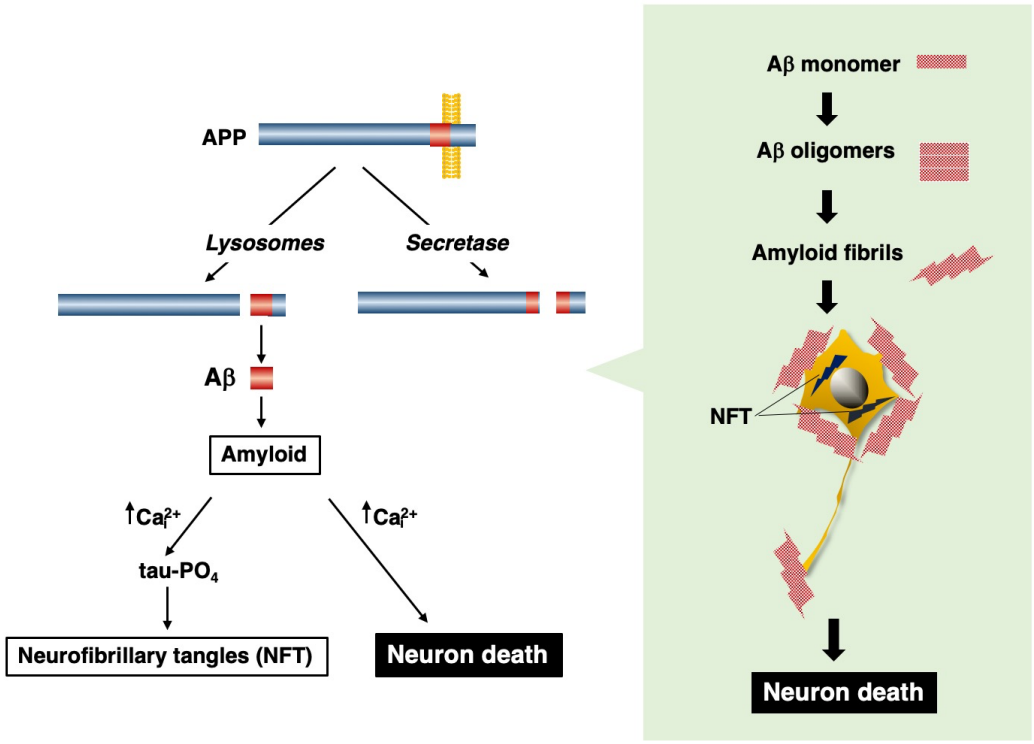

Figure 3. The amyloid cascade hypothesis. APP cleavage in the lysosomal compartment generates Aβ42 (*Aβ*) , whereas cleavage within the Aβ domain by secretase fails to generate Aβ42. The amyloid deposition in the extracellular space increases intraneuronal Ca^{2+} levels, leads to both NFT formation via tau phosphorylation, and induces neuron death. Aβ polymerizes to form amyloid fibrils, which are deposited near neurons and eventually cause neuron death. *Left panel*, adapted from Hardy and Higgins (1992).

Fig. 3 illustrates the amyloid cascade hypothesis reported originally by Hardy and Higgins (1992). APP is processed in the lysosomes into Aβ42 that polymerizes to form amyloid fibrils. If amyloid fibrils are neurotoxic, then formation of extracellular amyloid fibrils consisting of Aβ42 contributes to the pathogenesis of AD. However, there have been arguments as to whether Aβ *per se* exerts neurotoxicity (Yoshikawa, 1995). Furthermore, the amyloid cascade hypothesis raises the following questions: (1) How do neurons remain intact "for many years" despite the presence of growing

cytotoxic amyloid masses nearby? Should the amyloid burden be eliminated before its degenerative effect emerges? (2) How do dystrophic neurites form a cluster around the amyloid core of mature plaques? Does the amyloid core first attract neuronal processes and then deteriorate them? (3) Why do specific brain regions such as the hippocampus and association cortices, especially neocortical layers III and V, where large pyramidal neurons reside, contain more abundant APs than other brain regions? Do these regions have a larger number of specific loci where APs develop than other brain areas? To clarify these issues, we established APP-overexpressing cell models for studying the roles of APP in amyloidogenesis and neurodegeneration.

IV. Amyloidogenicity of APP-C100

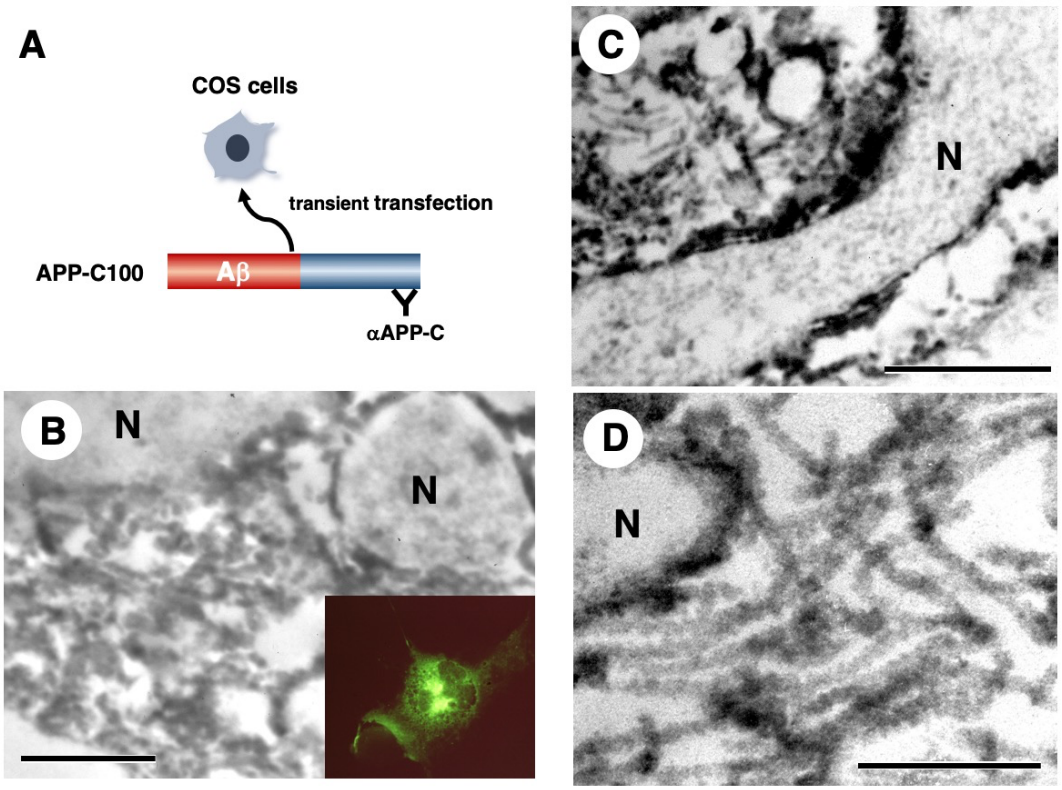

Figure 4. Amyloidogenicity of APP-C100. ***A***: Diagram of COS-1 cells transfected with human APP-C100 cDNA. APP-C100 cDNA was transiently transfected into COS-1 cells by DEAE-dextran method. ***B***: Electron micrograph of COS cells expressing APP-C100. Transfected COS cells were immunostained for APP C-terminal with an antibody to APP695 C-terminal peptide (*αAPP-C*) followed by detection with DAB peroxidase substrate. Ultrathin sections of selected cells showing intense immunoreactivity were observed by transmission electron microscopy. Fibrils near the nucleus (*N*) are darkly stained with immunoperoxidate reaction products, indicating the presence of APP-C100 in the amyloid-like fibrils. *Inset*, fluorescent micrograph of transfected COS cells accumulating APP-C100 near and on the nuclear membrane. ***C***, ***D***: Electron micrographs of sections stained with lead citrate and uranyl acetate. Amyloid-like fibrils with relatively homogenous diameters 15-22 nm are accumulated at the perinuclear region. *Scale bars*: 500 nm (in ***B***, ***C***), 200 nm (in ***D***). For experimental details, see Maruyama et al. (1990).

It remains unclear how and where amyloid fibrils are initially formed. The APP C-terminal 100 residues spanning the Aβ and cytoplasmic domains are prone to self-aggregate (Dyrks et al., 1988). To establish a cultured-cell model for amyloid fibril formation, we transiently transfected COS-I with cDNA encoding the carboxyl (C)-terminal 100 residues of human APP (APP-C100) (Fig. 4A)(Maruyama et al., 1990). Strong immunoreactivities for APP C-terminal (APP-C) are observed in a small population of APP-C100-transfected COS cells containing intracellular inclusion-like deposition in the perinuclear regions (inset in Fig. 4B). Immunoelectron microscopy reveals beaded or helical structures reacting with an antibody to APP-C (Fig. 4B). Electron microscopic observations of APP-C100-overexpressing COS cells demonstrate an accumulation of amyloid-like fibrils, designated "primordial amyloid fibrils" (Yoshikawa et al., 1991), with 8-22 nm diameter near the nuclear membrane (Fig. 4C, D). This suggests that formation of amyloid fibrils is an inherent characteristic of APP C-terminal fragments (APP-CTFs) encompassing the Aβ domain. In APP- C100 overexpressing COS cells, the primordial amyloid fibrils might be rapidly formed when large amounts of amyloidogenic APP-CTFs and scaffolds such as nuclear envelope are present. Thus, this cell model is useful for the molecular dissection of amyloidogenesis in AD.

V. Lysosomal dysfunction generates cytotoxic APP C-terminal fragments

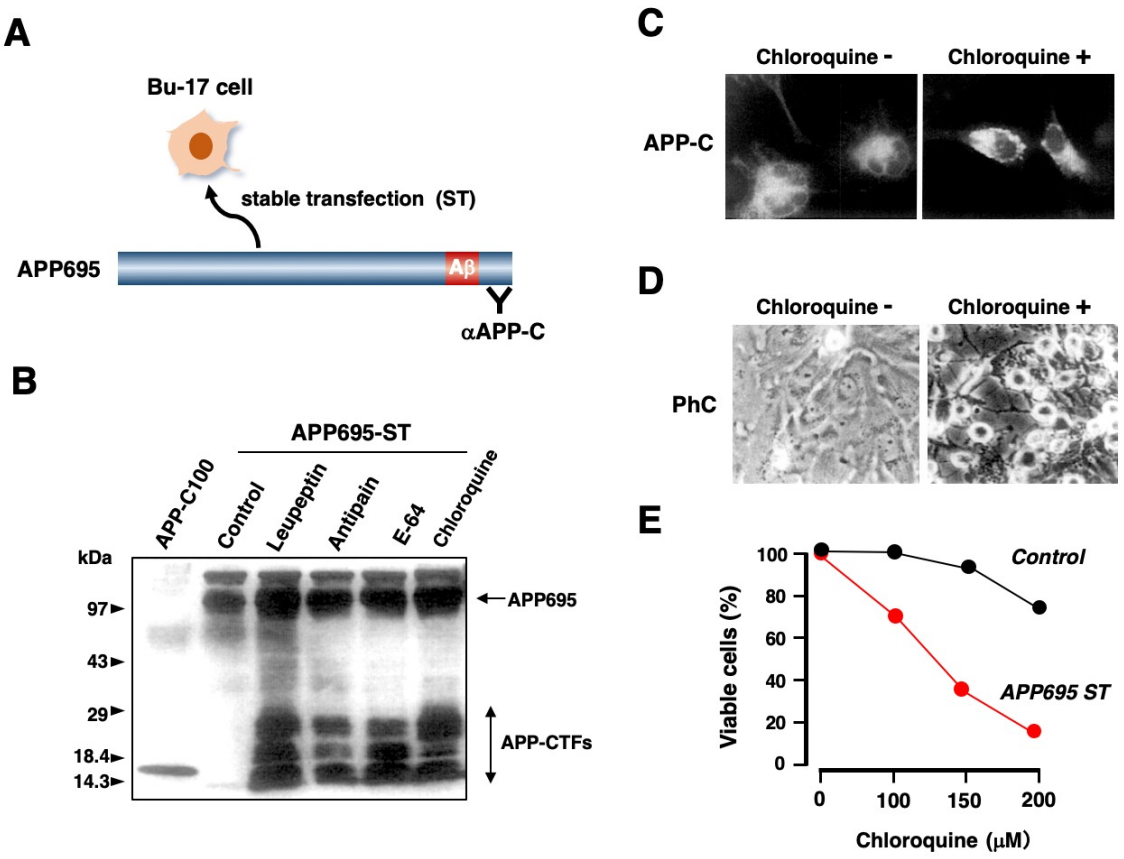

Figure 5. Lysosomal dysfunction generates cytotoxic APP C-terminal fragments. ***A***: Diagram of stable transfection (*ST*) of human wild-type APP695 cDNA into Bu-17 glioma cells. Bu-17 cells were stably transfected with full-length APP695 cDNA, cloned, and selected by immunostaining for high APP expression. ***B***: Effects of various protease inhibitors. Transfectants (*APP695-ST*) were treated for 24 h with leupeptin, antipain or E-64, and for 12 h with chloroquine. *Control*, no treatment. Molecular size makers are in kDa. *APP-C100* at 16 kDa. ***C***: Immunocytochemistry for APP. APP695-ST cells were treated for 24 h with (+) or without (-) chloroquine (100 μM) and immunostained for APP-C (*APP-C*). ***D***, ***E***: Cytotoxic effects of chloroquine. APP695-ST cells were treated with (+) or without (-) chloroquine (150 μM) for 3 days and observed by phase-contrast micrography (*PhC*) (***D***). APP695-ST cells and untransfected cells (*Control*) were treated for 3 days with chloroquine at indicated concentrations, and viable cells were counted (***E***). For experimental details, see Hayashi et al. (1992).

In an attempt to establish cell lines overexpressing APP-C100, we transfected APP-C100 cDNA into various cell lines including PC12 pheochromocytoma cells, P19 embryonal carcinoma (EC) cells, and glioma cells, but failed to obtain any clones expressing high levels of APP-C100 (Yoshikawa, 1993), suggesting that intracellular accumulation of APP-C100 is highly cytotoxic. We alternatively established stable transfectants expressing wild-type APP to examine whether cytotoxic APP-CTFs are generated by suppressing lysosomal activities. Human glioma cells (Bu-17), whose APP-secreting activity is low (Kametani et al., 1990), are stably transfected with wild-type human APP cDNA (Fig. 5A)(Hayashi et al., 1992). When treated with lysosomal protease inhibitors such as leupeptin, antipain, E-64, and chloroquine, a compound reducing the lysosomal activity, these transfectants accumulate APP-CTFs (larger than APP-C100 at 16 kDa) (Fig. 5B). The APP-C immunoreactivity is localized in lysosome-like organelles when treated with chloroquine (Fig. 5C). These transfectants exhibit degenerative changes when treated with chloroquine (Fig. 5D, E), suggesting that APP-CTFs generated in the lysosomes are cytotoxic.

VI. Degeneration *in vitro* of postmitotic neurons overexpressing wild-type APP

Murine P19 EC cells are pluripotent stem cells that differentiate efficiently into postmitotic neurons (McBurney et al., 1982). P19 EC cells treated with retinoic acid (RA) differentiate into neurons and glial cells, and these cells express different species of APP (Yoshikawa et al., 1990). P19 EC cells are stably transfected with human full-length APP cDNA and differentiated into postmitotic neurons by RA treatment (Fig. 6A)(Yoshikawa et al., 1992). RA-treated P19 EC cells express APP695 initially and then APP751/770 (Fig. 6B). These changes of APP species correspond to the differentiation patterns of neurons and astrocytes (Yoshikawa et al., 1990). When human wild-type APP cDNA-transfected P19 EC cells are treated with RA, neurons undergo severe degeneration and contain APP-CTFs that encompass the entire Aβ domain (larger than APP-C100, >16 kDa)(Fig. 6C). Most of the degenerating neurons disappear in a few days, whereas non-neuronal cells show no degeneration (Fig. 6D). These results suggest that postmitotic neurons are highly vulnerable to overexpression of APP, which undergoes aberrant processing into amyloidogenic APP-CTFs. Neither conditioned media of APP695 cDNA-transfected cells (P19, Bu-17) nor APP-C100 purified from APP-C100 cDNA-transfected E. Coli shows neurotoxicity when applied extracellularly (Yoshikawa, 1995), indicating that these APP cDNA-transfectants are vulnerable to “intracellular” amyloidogenic APP-CTFs. Overexpression of wild-type human APP695 also induces degeneration of N2a cells, a mouse neuroblastoma cell line derived from the neural crest (Lu et al., 2000).

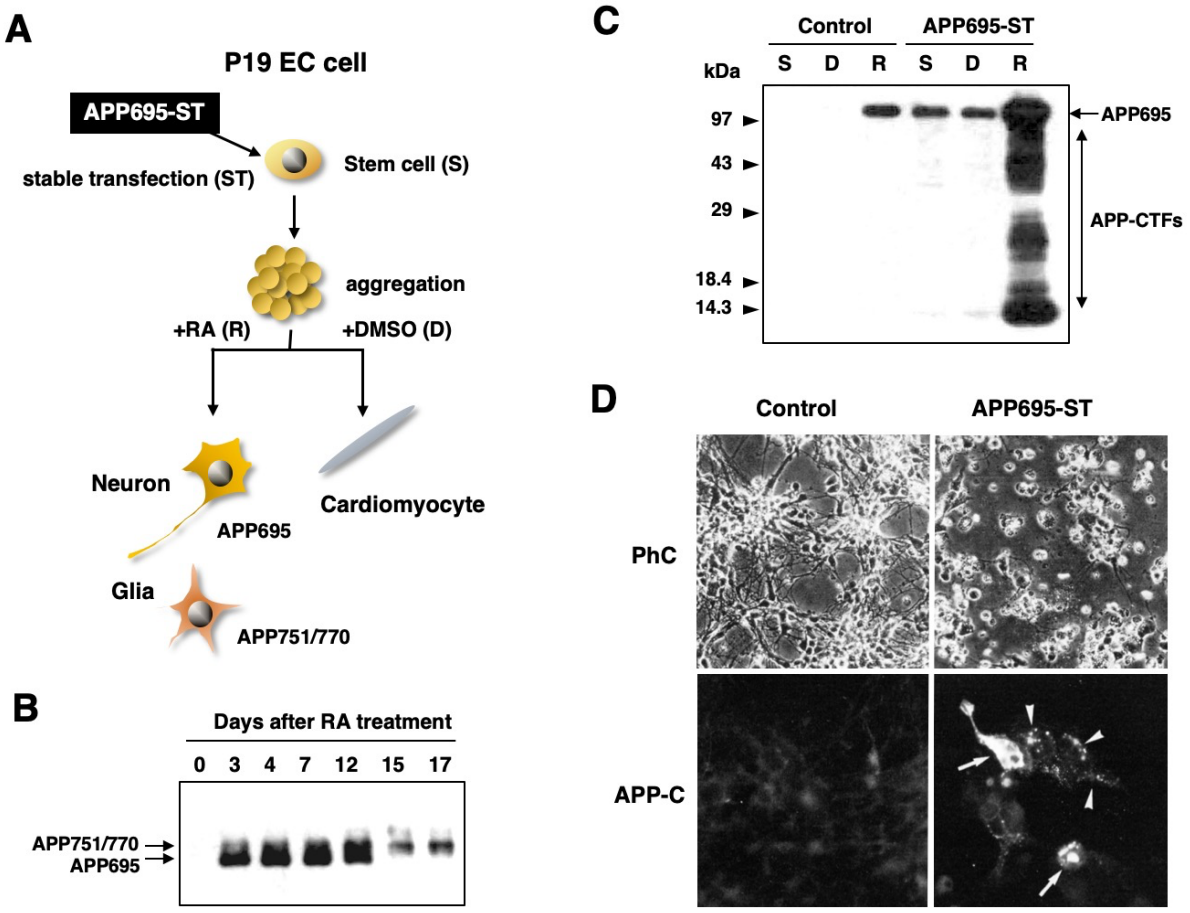

Figure 6. Degeneration *in vitro* of postmitotic neurons overexpressing wild-type APP. ***A***: Diagram of murine P19 embryonal carcinoma (EC) cells. Cells are aggregated and treated with retinoic acid (*RA*) for neural differentiation. Treatment with dimethyl sulfoxide (*DMSO*) induces differentiation into cardiomyocytes. Human wild-type APP695 is stably transfected (*ST*) into P19 EC stem cells. ***B***: Endogenous expression of APP in P19 EC cells. P19 EC cells were cultured for indicated durations after RA treatment, and APP in cell lysates was analyzed by immunoblotting for APP-C. APP bands corresponding to APP695 at 105-120 kDa are predominant during neuronal differentiation (days 3-12), and those corresponding to APP751/770 at 115-130 kDa during glial differentiation (days 15 and 17) after neuronal disappearance. ***C***: Immunoblots of APP695 cDNA-transfected P19 cells. APP in cell lysates was analyzed by immunoblotting for APP-C. Abundant APP-CTFs at 16-97 kDa are generated in APP695-ST cells treated with RA. *Control,* empty vector-transfected P19 cells; *APP695-ST*, APP695 cDNA stably transfected cells; *S*, stem cells; *D*, DMSO-treated cells; *R*, RA-treated cells. ***D***: Degeneration of APP695-ST-derived neurons. APP695-ST cells were treated with RA and incubated for another 4 days. *Upper panels*: phase-contrast micrographs (*PhC*) of control and APP695-ST cells. *Lower panels*: fluorescent immunocytochemistry for APP-C (unpublished data). In APP695-ST cells, APP-C immunoreactivity is intense in degenerating neurons (*arrows*), but spotty, presumedly lysosomal, in non-neuronal cells (*arrowheads*). For experimental details, see Yoshikawa et al. (1992).

VII. The internal disintegration hypothesis

The author proposed a hypothesis based on the analyses of APP-overexpressing cell models for APP-induced AD pathogenesis (Yoshikawa, 1995). Fig. 7 illustrates the hypothesis for neuronal

internal disintegration as a result of intraneuronal accumulations of APP and amyloidogenic APP-CTFs. Postmitotic neurons express high levels of APP695 from the early period of terminal differentiation (Yoshikawa et al., 1990). Thus, each neuron must possess high capability of metabolizing a large amount of APP into nontoxic fragments for maintaining the healthy state (Phase I). Overexpression of APP and reduced lysosomal function lead to the abnormal metabolism of APP in neurons where amyloidogenic APP-CTFs start to accumulate in the lysosomes (Phase II). During this period, Aβ is deposited around compromised neurons and their neurites to form diffuse plaques. When accumulations of APP and APP-CTFs reach critical levels, compromised neurons start to disintegrate (Phase III). During neuronal degeneration, amyloidogenic APP-CTFs encompassing the Aβ domain form intraneuronal primordial amyloid fibrils. These initial amyloids are converted to mature amyloid fibrils at the extracellular space. After degenerated neurons are completely scavenged by glial cells, only amyloid masses and surrounding dystrophic neurites remain at the extracellular space. Dystrophic neurites in neuritic plaques are presynaptic nerve terminals that miss their target neurons.

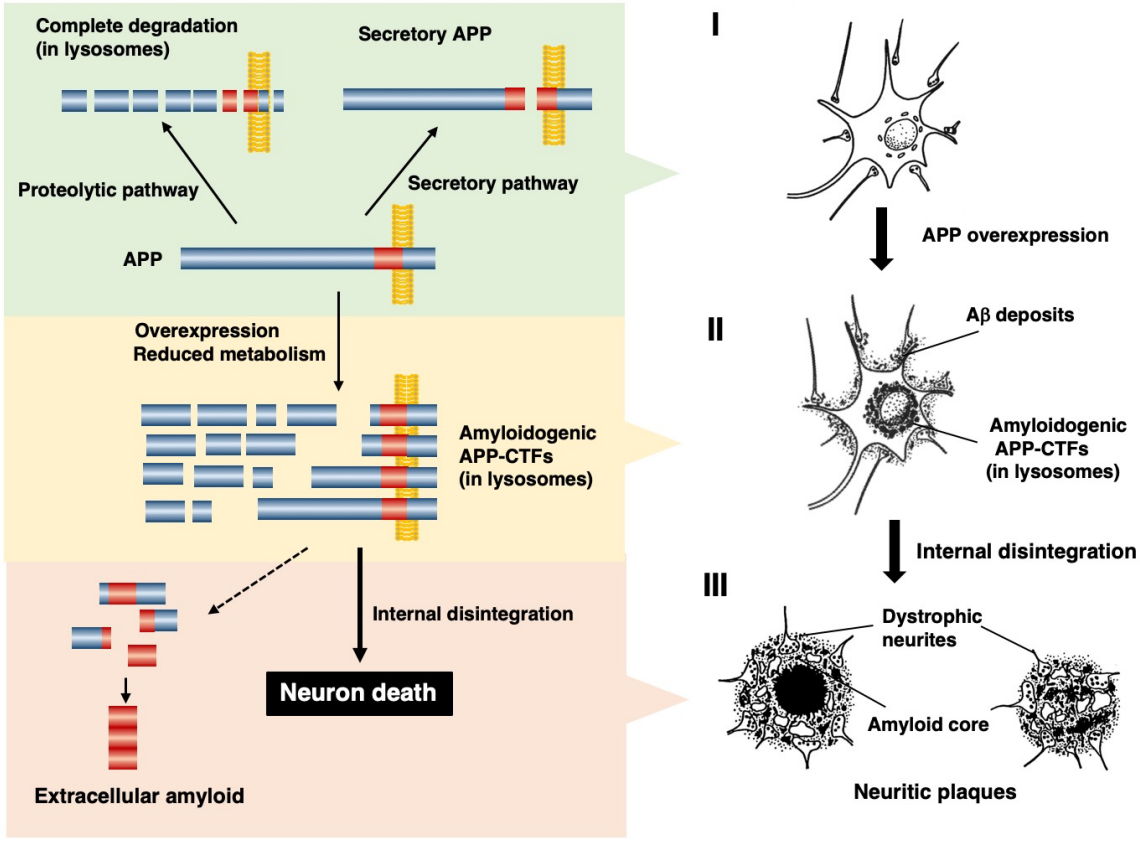

Figure 7. The internal disintegration hypothesis. Hypothetical explanation for neuronal degeneration and neuritic plaque formation in AD on the basis of analytical data on APP-overexpressing cell models (Yoshikawa 1995). *Phase I*: A healthy neuron metabolizes APP completely. Overexpression of APP and reduction of APP metabolism lead to accumulation of APP and APP-CTFs in the lysosomes. *Phase II*: When the intracellular accumulations of APP and APP-CTFs reach critical levels, compromised neurons undergo degeneration via internal disintegration. Amyloidogenic APP-CTFs are processed further into Aβ that eventually forms mature amyloid fibrils. *Phase III*: At the final stage of neuronal degeneration, amyloid deposits and dystrophic neurites remain at the extracellular space after neuronal disappearance. Illustrations adapted from Yoshikawa (1995). For preliminary report, see Yoshikawa (1993).

VIII. Activation of Csp3 in human neurons overexpressing wild-type APP

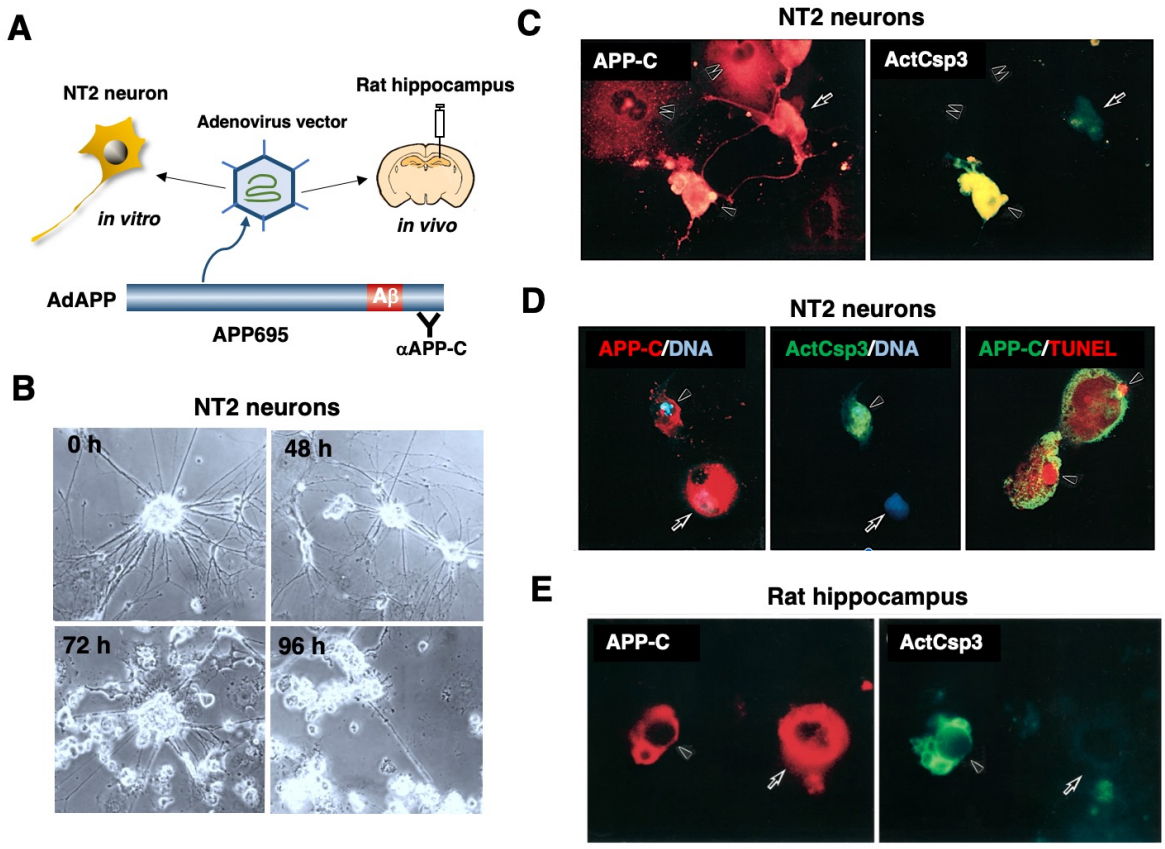

Figure 8. Activation of Csp3 in human neurons overexpressing wild-type APP. ***A***: Diagram of adenovirus vector-mediated APP overexpression. Human NT2 EC cells are differentiated into postmitotic neurons by RA treatment. Recombinant adenovirus carrying human wild-type APP695 (*AdAPP*) was infected into NT2-derived neurons (*NT2 neurons*) *in vitro*, or directly injected into rat hippocampus *in vivo*. ***B***: Phase-contrast micrographs of AdAPP-infected NT2 neurons. Infected neurons show intact morphology until 48 h, start to degenerate at 72 h, and exhibit severe degeneration at 96 h. ***C***: Fluorescent immunocytochemistry of AdAPP-infected NT2 neurons. Infected NT2 neurons were fixed at 72 h after viral infection and double-immunostained for APP-C and activated Csp3 (*ActCsp3*). ***D***: Apoptotic nuclei in AdAPP-infected NT2 neurons. AdAPP-infected NT2 neurons were double-labeled for APP-C/DNA, ActCsp3/DNA, and APP-C/TUNEL (merged images in each panel in ***D***). *TUNEL*, staining for DNA fragmentation. Chromosomal DNA (*blue*) was stained with Hoechst 33342. **E**: Fluorescent immunohistochemistry for APP and ActCsp3. AdAPP-infected rat hippocampal tissues (*Rat hippocampus*) were fixed *in vivo* at 72 h and immunostained for APP-C and ActCsp3. In ***C***-***E***, *arrowheads* point to APP-accumulating apoptotic neurons with intense ActCsp3 immunoreactivity, *arrows* to compromised neurons, *double-arrowheads* (in ***C***) to intact non-neuronal cells. For experimental details, see Uetsuki et al. (1999)

A question arises as to whether the reduced number of APP-overexpressing P19 EC cell-derived neurons is not attributed to APP-induced neuronal death but to impaired neuronal differentiation of P19 EC cells. To answer it, APP is overexpressed in postmitotic neurons after complete terminal differentiation of human NT2 EC cells (Andrews, 1984), which, like P19 EC cells, differentiate efficiently into postmitotic neurons by RA treatment. We employed a recombinant adenovirus system which is efficiently infected into postmitotic neurons both *in vitro* and *in vivo* (Fig. 8A) (Uetsuki et al., 1999). When the recombinant adenovirus carrying human wild-type APP695 cDNA

is infected *in vitro* into NT2-derived postmitotic neurons, they undergo severe degeneration (Fig. 8B). Caspase-3 (Csp3) is a principal protease involved in neuronal apoptosis during physiological development and under pathological conditions. Immunocytochemical analyses reveal that some of APP-accumulating neurons contain activated Csp3 and exhibit the characteristics of apoptosis such as nuclear shrinkage, chromatin condensation, DNA fragmentation (TUNEL-positive), and plasma membrane blebbing (Fig. 8C, D). Activation of Csp3 and apoptotic changes are also observed *in vivo* in rat hippocampal neurons infected with the APP-expressing adenovirus (Fig. 8E). These results imply that overexpression of wild-type APP in postmitotic neurons induces Csp3-mediated apoptosis.

IX. Degeneration *in vivo* of hippocampal neurons overexpressing wild-type APP

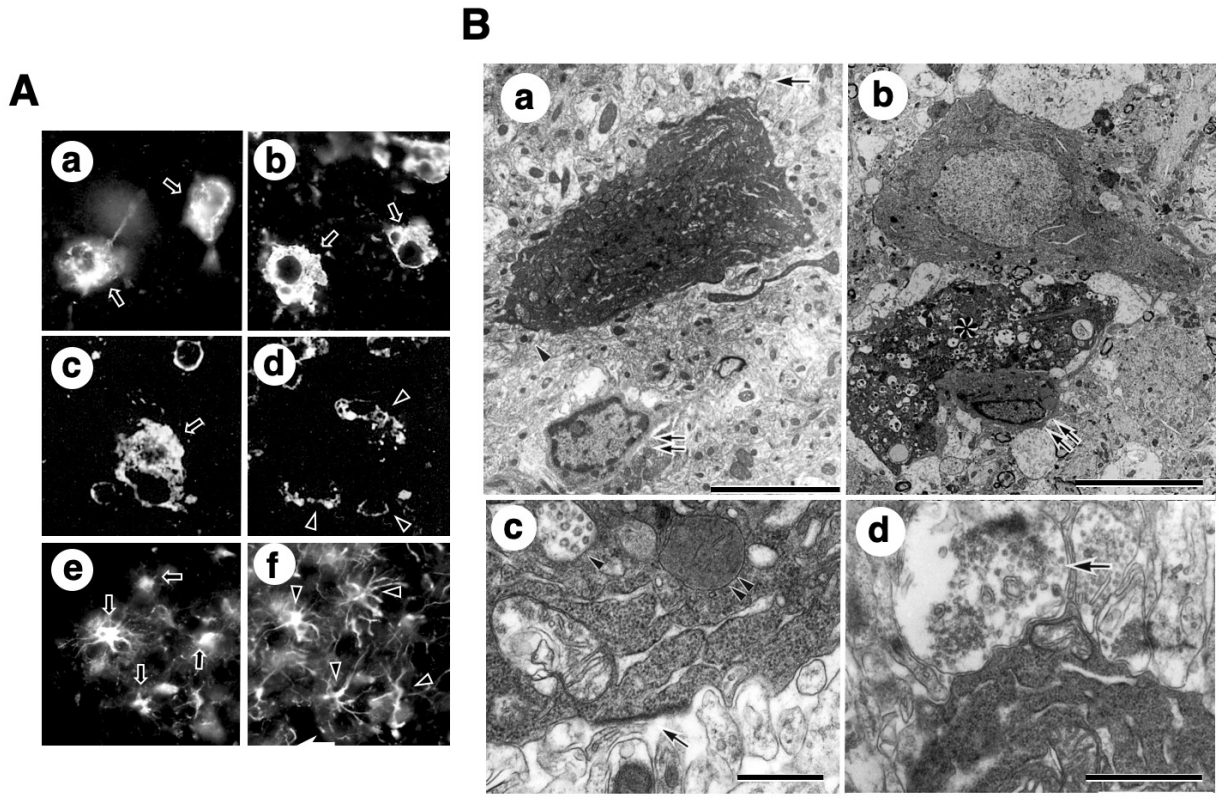

Figure 9. Degeneration *in vivo* of hippocampal neurons overexpressing wild-type APP. ***A***: Degeneration of APP-accumulating hippocampal neurons. AdAPP was directly injected into rat dorsal hippocampus *in vivo* as in Fig. 8A. Hippocampal tissues were immunostained for APP-C on day 4. Degenerating neurons contain strongly APP-immunoreactive materials in the perikarya (***a***) and show plasma membrane blebbing (***b***). Cryosections were double-labeled by fluorescent immunohistochemistry for APP-C (***c***) and the microglial marker Griffonia lectin (***d***) or double-immunostained for APP-C (***e***) and the astrocyte marker GFAP (**f**). Microglial cells (*arrowheads* in ***d***) and astrocytes (*arrowheads* in ***f***) are adjacent to APP-accumulating degenerating neurons (*arrows* in ***c***, ***e***). ***B***: Electron micrographs of degenerating neurons in AdAPP-infected hippocampus. Hippocampal tissues were prepared 4 day after AdAPP infection and examined by electron microscopy. Areas indicated by *arrowhead* and *arrow* in ***a*** are enlarged in ***c*** and ***d***, respectively. Abnormalities such as electron-dense cytoplasm (***a***, ***b***), numerous clear vacuoles (*asterisk* in ***b***), multivesicular bodies (*arrowhead* in ***c***), dense bodies *(double-arrowhead* in ***c***), swollen presynaptic ending (*arrow* in ***d***), and postsynaptic density lacking presynaptic element (*arrow* in ***c***). Microglial cells are adjacent to degenerating neurons (*double-arrows* in ***a***, ***b***). Scale bars: ***a***, 5 μm; ***b***, 10 μm; ***c***, 500 nm; ***d***, 1 μm. For experimental details, see Nishimura et al. (1998)

To examine the morphological characteristic of APP-accumulating postmitotic neurons *in vivo*, full-length APP695 cDNA was introduced into rat hippocampal neurons using the recombinant adenovirus vector system (Nishimura et al., 1998). When the recombinant adenovirus carrying wild-type human APP695 cDNA is injected *in vivo* into the hippocampus, some of infected neurons in the hippocampus undergo severe degeneration in a few days. Degenerating neurons with strong APP-C immunoreactive materials near the nuclei exhibit deformed somata and plasma membrane blebbing (Fig. 9Aa,b). Microglial cells and astrocytes are often observed near APP-overexpressing degenerating neurons (Fig. 9Ac-f). Although these degenerating neurons accumulate APP or APP-CTFs, Aβ-immunoreactive materials are undetected in the extracellular space. Electron microscopic examinations reveal that degenerating neurons have shrunken perikarya along with synaptic abnormalities (Fig. 9Ba-d). Microglial cells are often found in close proximity to degenerating neurons and, in some cases, phagocytose these neurons. These results suggest that intracellular accumulation of full-length APP695 induces neuronal degeneration *in vivo* in the absence of extracellular Aβ deposition.

X. Activation of calpain in human neurons overexpressing APP

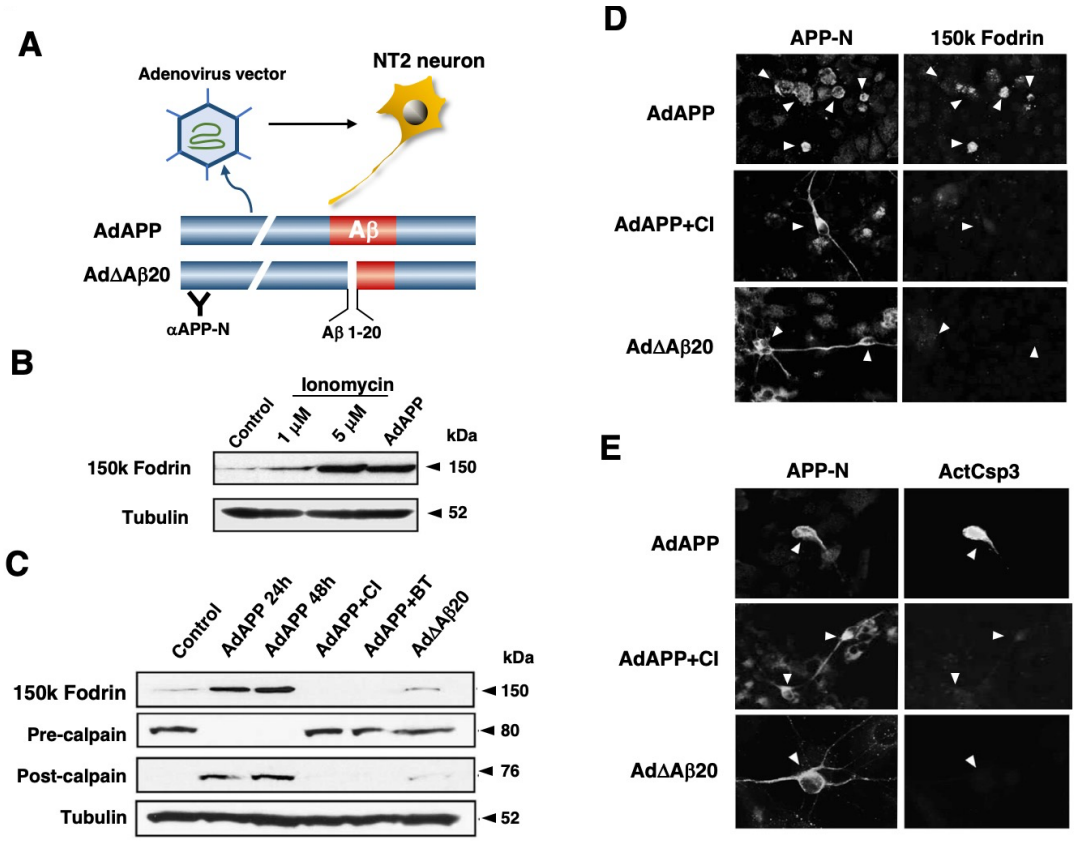

Figure 10. Activation of calpain in human neurons overexpressing APP. ***A***: Diagram of adenovirus vector-mediated expression of APP695 (*AdAPP*) and APP mutant lacking Aβ(1-20) (*AdΔAβ20*). AdAPP and AdΔAβ20 were infected *in vitro* into cultured NT2 neurons. ***B***: Cleavage of α-fodrin by ionomycin and APP overexpression. NT2 neurons were treated with the calcium-ionophore ionomycin or infected with AdAPP. Cell extracts were analyzed by immunoblotting using antibodies to calpain-cleaved 150 kDa α-fodrin fragment (*150k Fodrin*) and β-tubulin (*Tubulin*). *Control*, no viral infection. ***C***: Effects of calpain inhibitors. NT2 neurons were infected with AdAPP and AdΔAβ20. AdAPP-infected cells were incubated in the presence of calpain inhibitor I (*CI*) or BAPTA-AM (*BT*). Cell extracts were analyzed by immunoblotting for 150k fodrin, 80 kDa pre-autolytic μ-calpain (*Pre-calpain*), 76 kDa post-autolytic μ-calpain (*Post-calpain*) and β-tubulin. ***D***: Accumulation of 150k fodrin in APP-overexpressing neurons. NT2 neurons were infected with AdAPP and AdΔAβ20, treated with calpain inhibitor I (*AdAPP+CI*), fixed 48 h later, and double-immunostained for APP-N and 150k fodrin. ***E***: Inhibition of APP-induced Csp3 activation by CI. NT2 neurons were infected with AdAPP and AdΔAβ20, treated with CI, fixed 48 h later, and double-immunostained for APP-N and activated Csp3 (*ActCsp3*). AdAPP-induced Csp3 activation is protected by CI, and neither calpain nor Csp3 is activated by AdΔAβ20 infection. For experimental details, see Kuwako et al. (2002).

We next investigated the mechanism of APP-induced Csp3 activation using NT2 EC cell-derived postmitotic neurons and adenovirus vector system (Fig. 10A)(Kuwako et al., 2002). In this system, overexpression of wild-type APP by adenovirus infection increases intraneuronal Ca^{2+} levels and Csp3 activation. The Ca^{2+} ionophore ionomycin and adenovirus-mediated APP overexpression increase the levels of calpain-cleaved 150 kDa α-fodrin fragment (Fig. 10B). Overexpression of APP induces autolysis-dependent activation of calpain by detecting the appearance of post-autolytic μ-calpain 76 kDa fragment and disappearance of pre-autolytic μ-calpain 80k fragment (Fig. 10C). Calpain inhibitors such as calpain inhibitor I and BAPTA-AM almost completely suppress the activation of calpain. Neither calpain nor Csp3 is activated in neurons expressing the Aβ(1–20) domain-defective APP mutant. Adenovirus-mediated APP overexpression increases immuno-reactivities for cleaved 150 kDa α-fodrin (Fig. 10D) and activated Csp3 (Fig. 10E). These immunoreactivities are suppressed by the calpain inhibitors, and the Aβ(1–20) domain-defective APP mutant fails to increase these immunoreactivities. These results suggest that overexpression of wild-type APP activates calpain that mediates Csp3 activation in postmitotic neurons. Thus, APP overexpression in postmitotic neurons increases intracellular Ca^{2+} levels and induces a sequential activation of the Ca^{2+}-dependent protease calpain and the apoptosis-executioner protease Csp3, indicating that calpain activation precedes Csp3 activation.

XI. Csp3-cleaved APP (APPΔC31) induces apoptosis

Activated caspases cleave APP to generate its C-terminal-truncated fragment (APPΔC31) (Gervais et al., 1999; Lu et al., 2000). We examined whether APPΔC31 is generated in APP-overexpressing postmitotic neurons (Nishimura et al., 2002). MAP2-immunoreactive NT2 neurons exhibit apoptotic features such as nuclear fragmentation and condensation after serum deprivation (Fig. 11B). These apoptotic neurons contain both activated Csp3 and APPΔC31. To examine whether APPΔC31 *per se* affects neuronal viability, we constructed an APPΔC31-expressing adenovirus vector and infected it into NT2 neurons (Fig. 11A, C). APPΔC31-expressing neurons undergo apoptotic changes as analyzed by TUNEL assay for DNA fragmentation, but activated Csp3 is undetected in these cells, suggesting that APPΔC31 induces apoptosis in a Csp3-indendent manner. A number of neurons expressing APPΔC31 and APP undergo death as analyzed by EthD-1

retention test, whereas wild-type APP fails to induce death of NT2 stem cells (Fig. 11D, E). APPΔC31 lacking the Aβ(1-20) domain exerts no cytotoxic effects (Nishimura et al., 2002). These findings suggest that accumulation of wild-type APP activates neuronal Csp3 to generate APPΔC31 which mediates apoptosis in both neuronal and non-neuronal cells.

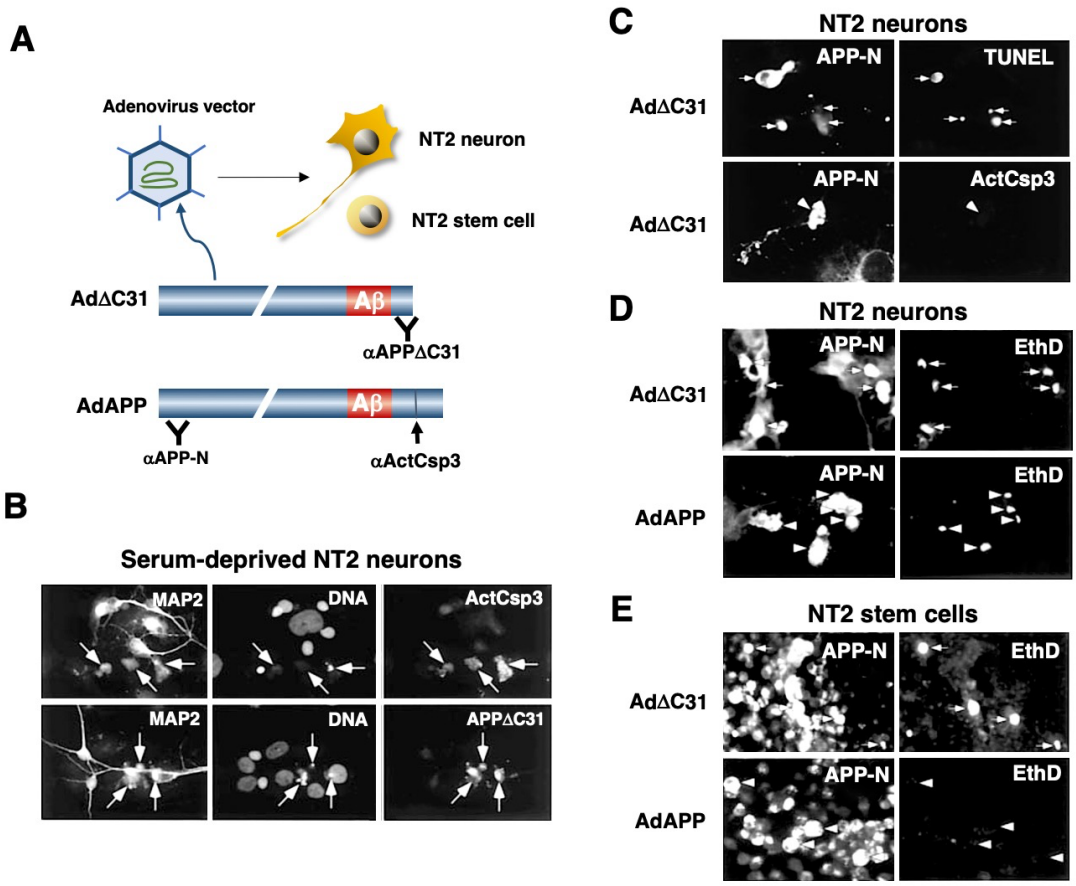

Figure 11. Csp3-cleaved APP (APPΔC31) induces apoptosis. ***A***: Diagram of adenovirus vector-mediated expression of full-length APP695 (*AdAPP*) and APP lacking APP-C31 (*AdΔC31*). AdAPP and AdΔC31 were infected into cultured NT2 stem cells and NT2 neurons. ***B***: Csp3 activation and APPΔC31 generation in NT2 neurons by serum deprivation. NT2 neurons were incubated for 96 h in the absence of fetal calf serum, and triply labeled for the neuron marker MAP2, chromosomal DNA, and ActCsp3 or APPΔC31. *Arrows* point to apoptotic neurons containing ActCsp3 and APPΔC31. ***C***: Expression of APPΔC31 induces apoptosis in a Csp3-independent manner. NT2 neurons were infected with AdΔC31 and double-labeled for APP-N and TUNEL or ActCsp3. *Arrowhead* points to ActCsp3-negative apoptotic neurons. ***D***: Death of NT2 neurons infected with AdAPP and AdΔC31. Neurons were fixed 72 h after infection and double-labeled for APP-N and cell death indicator (*EthD*). Both AdAPP and AdΔC31 induce death of NT2 neurons. ***E***: Death of NT2 stem cells infected with AdΔC31. NT2 stem cells were fixed 72 h after infection and double-labeled for APP-N and EthD. NT2 stem cells undergo death by AdΔC31 (*arrows*), but not by AdAPP (*arrowheads*). For experimental details, see Nishimura et al. (2002).

XII. Sequential events in APP-induced neuronal apoptosis

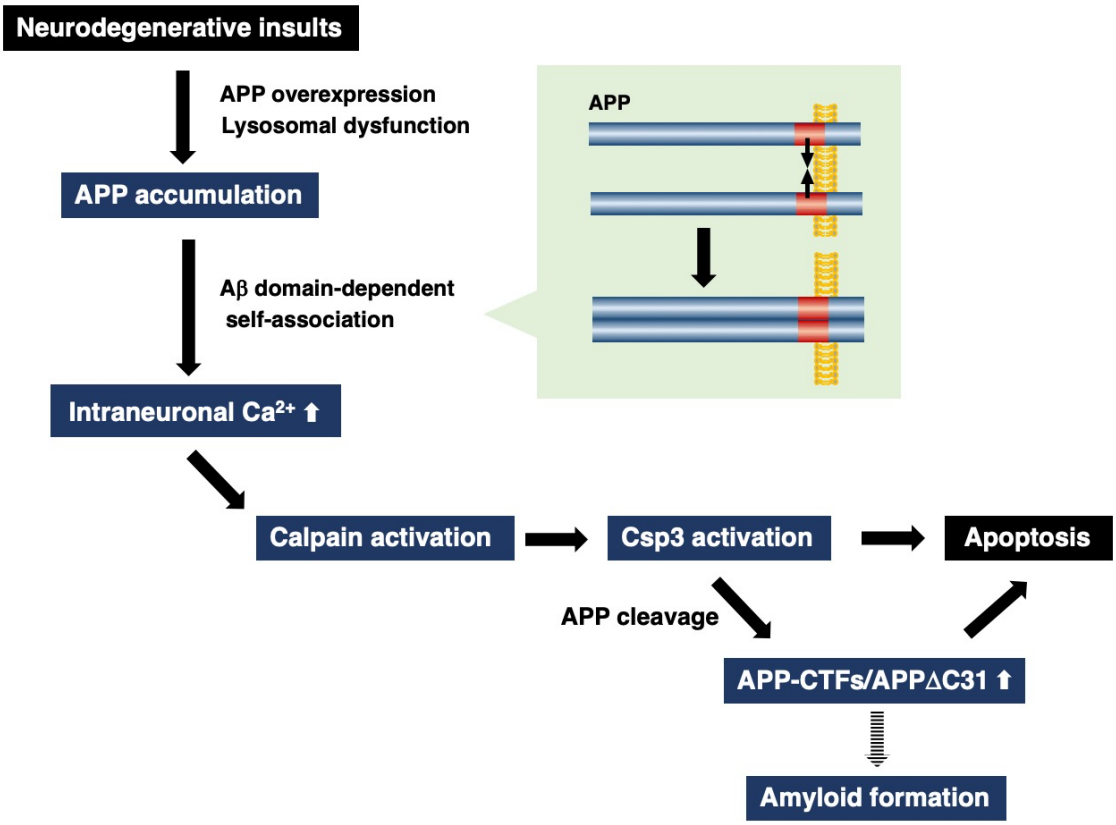

Figure 12. Sequential events in APP-induced neuronal apoptosis. Neurodegenerative insults induce APP overexpression and APP accumulation which is promoted by lysosomal dysfunction. Accumulated APP undergoes dimerization, elevates intraneuronal Ca^{2+} levels, and triggers the calpain-Csp3 pathway for apoptosis. Csp3 cleaves APP into APPΔC31 that propels the apoptotic process. See text for explanation.

A model for the molecular mechanism that induces apoptosis in APP-overexpressing neurons is schematized in Fig. 12. APP overexpression induced by neurodegenerative insults and lysosomal dysfunction promotes intraneuronal APP accumulation, which causes Aβ-domain-dependent APP dimerization as demonstrated by a cross-linking experiment (Nishimura et al., 2002). In addition, a monoclonal antibody (22C11) reacting with an APP N-terminal sequence induces neuronal apoptosis (Rohn et al., 2000; Nishimura et al., 2003). Adenovirus vector-mediated APP over-expression increases intraneuronal Ca^{2+} levels (Tominaga et al., 1997; Kuwako et al., 2002) and induces the sequential activation of calpain and Csp3. Activated Csp3 executes apoptosis by cleaving several proteins, of which APP serves as a substrate. APP is cleaved into APPΔ31, which *per se* induces apoptosis in a Csp3-independent manner. Both calpain and Csp3 are likely involved in the accumulation of APP-CTFs that form primordial amyloid fibrils in compromised neurons.

XIII. APP increases in sensory neurons during apoptosis

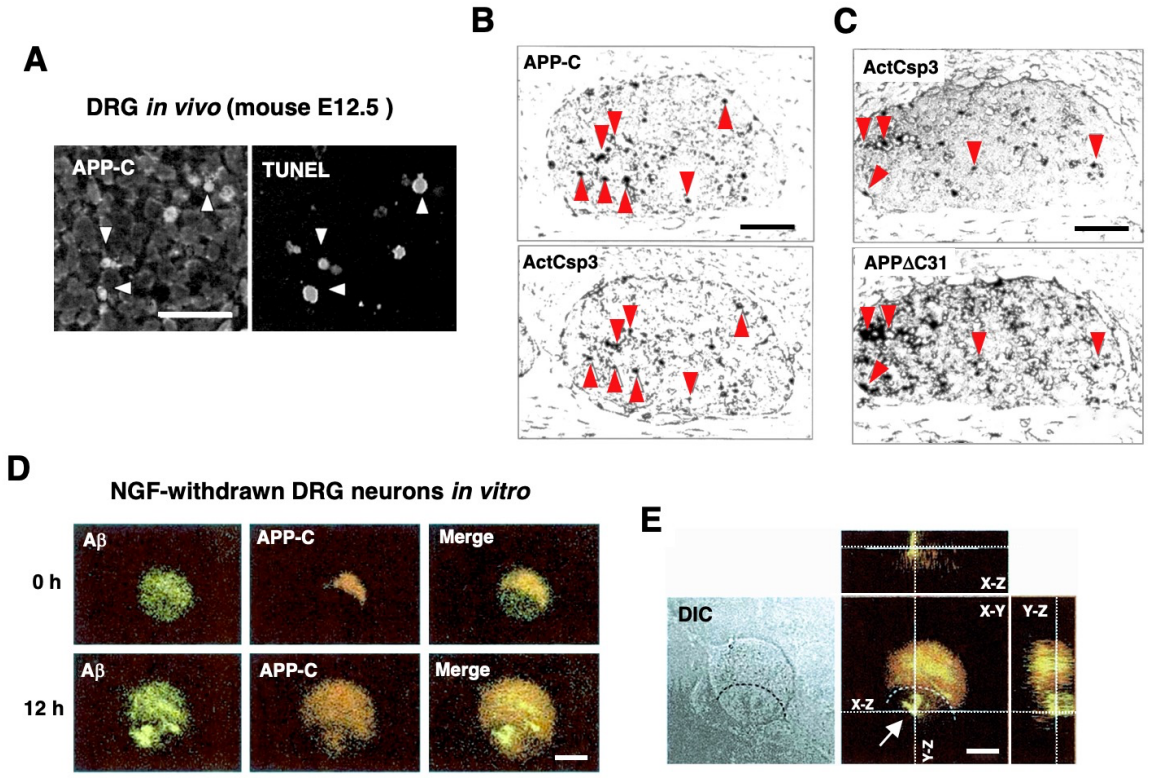

Figure 13. APP increases in sensory neurons during apoptosis. ***A***: APP upregulation *in vivo* during developmental apoptosis of DRG sensory neurons. Mouse DRG at embryonic day 12.5 (E12.5) was isolated and double-labeled for APP-C and TUNEL. *Arrowheads* point to TUNEL-positive apoptotic cells with high APP-C immunoreactivity. ***B***, ***C***: APP-C, ActCsp3 and APPΔC31 in DRG *in vivo*. Adjacent sections of mouse E12.5 DRG were immunostained for APP-C/ActCsp3 (***B***) and ActCsp3/APPΔC31 (***C***). *Arrowheads* (*red*) point to cells with high levels of APP-C, ActCsp3 and APPΔC31. ***A***-***C***; unpublished data. ***D***: Accumulation of Aβ and APP-C in NGF-deprived DRG neurons *in vitro*. DRG neurons were prepared from E12.5 mice, treated with NGF for 36 h, immunostained for Aβ and APP-C at *0 h* and *12 h* after NGF withdrawal, and observed by confocal laser scanning microscopy. ***E***: Three-dimensional images of Aβ and APP-C. Images are merged for three-dimensional presentation. Note the Aβ/APP-C-immunoreactive aggregates in the nucleus (*arrow*). Differential interference contrast (*DIC*) and merged images in X-Z and Y-Z axes are shown in accessory panels. Scale bars; 100 μm (***A***-***C***), 10 μm (***D***, ***E***). For experimental details, see Nishimura et al. (2003).

APP mRNA and protein levels are elevated during programmed death of spinal motor neurons, in which APP serves as a Csp3 substrate (Barnes et al., 1998). To examine the expression and role of intraneuronal APP in programmed neuronal death, we employed the dorsal root ganglion (DRG), a typical organ where programmed developmental death occurs (Nishimura et al., 2003). At E12.5, APP-overexpressing neurons are labeled with TUNEL for apoptosis-specific DNA fragmentation in DRG *in vivo* (Fig. 13A), indicating a link between APP overexpression and apoptosis of DRG neurons. DRG cells contain high levels of APP/activated Csp3 (Fig. 13B) and activated Csp3/APPΔC31 (Fig. 13C), indicating APP-induced Csp3-dependent apoptosis occurs during DRG development. Nerve growth factor (NGF) promotes differentiation and survival of sensory neurons

in DRG, and withdrawal of NGF induces neuronal death (apoptosis). When primary cultures of DRG cells prepared from mouse embryos are treated with NGF, neuronal APP levels are elevated (Nishimura et al., 2003). Remarkably, APP also increases in NGF-withdrawn DRG neurons. Immunoreactivities for both Aβ and APP-C are elevated in DRG neurons at 12 h after NGF-withdrawal (Fig.13D). At this stage, amorphous aggregates immunoreactive for both Aβ and APP-C, presumably those of APP-CTFs, are present in the cytoplasm and nucleus (Fig. 13E).

XIV. APP plays a dual role in sensory neuron viability during apoptosis

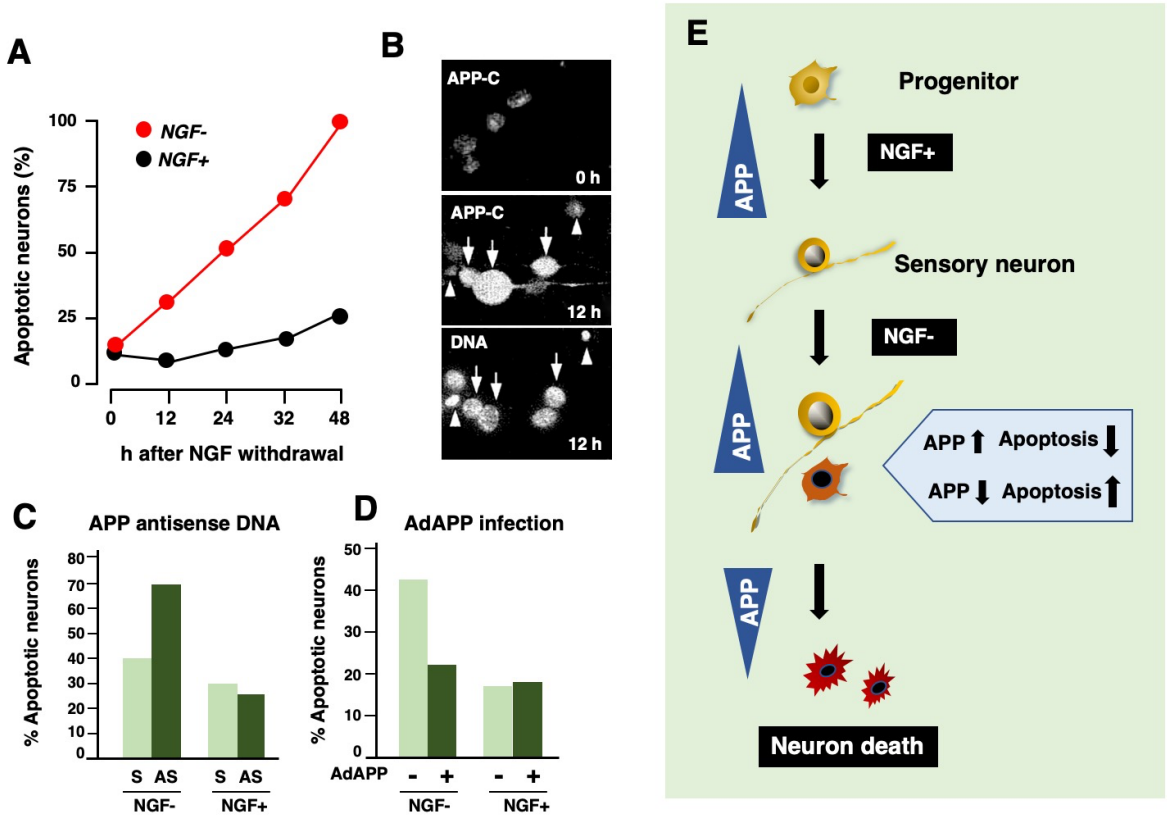

Figure 14. APP plays a dual role in sensory neuron viability during apoptosis. ***A***: Apoptosis of DRG neurons by NGF deprivation. DRG neurons were prepared from E12.5 mice, treated with NGF for 36 h, fixed at indicated times after NGF withdrawal, and labeled for MAP2 and chromosomal DNA. MAP2-positive neurons bearing apoptotic nuclei were counted. ***B***: Upregulation of APP in NGF-deprived DRG neurons. Neurons were immunostained for APP-C at *0 h* and *12 h* after NGF withdrawal and double-labeled for APP-C (*APP-C*) and chromosomal DNA (*DNA*) at 12 h. APP-C immunoreactivity is strong in cells with intact morphology (*arrows*) but low in cells with apoptotic nuclei (*arrowheads*). ***C***: Enhanced apoptosis of NGF-deprived DRG by APP reduction. DRG neurons were incubated for 24 h in the absence (*NGF-*) and presence (*NGF+*) of NGF in the medium containing APP sense (*S*) and antisense (*AS*) oligonucleotides, and stained with Hoechst 33342 for apoptotic nuclei. ***D***: Reduced apoptosis in NGF-deprived DRG neurons by APP overexpression. DRG neurons were infected with AdAPP (*AdAPP+*) or control LacZ-expressing adenovirus (*AdAPP-*) and incubated for 24 h in the absence and presence of NGF. Cells were double-labeled for MAP2 and Hoechst 33342 for apoptotic nuclei. ***E***: Dual role of APP in DRG neuron viability. APP plays a dual role in the regression and progression of apoptosis at the early stage, but APP levels in NGF-deprived neurons decrease at the late stage of apoptosis. For experimental details and statistical data, see Nishimura et al. (2003).

When NGF is withdrawn from DRG cultures after NGF treatment, the number of apoptotic neurons is markedly increased, and virtually all neurons undergo apoptosis at 48 h (Fig. 14A) (Nishimura et al., 2003). At 12 h after NGF withdrawal, DRG neurons with intact morphology express high levels of APP, and those carrying apoptotic nucleus contain much less APP (Fig. 14B). APP antisense oligonucleotide-induced reduction of endogenous APP significantly increases the number of apoptotic neurons (Fig. 14C), whereas adenovirus-mediated APP overexpression reduces neuronal apoptosis (Fig. 14D). These results suggest that endogenous APP is upregulated to exert an anti-apoptotic effect on NGF-deprived DRG neurons and subsequently undergoes Csp3-dependent proteolysis during apoptosis. As summarized in Fig. 14E, APP plays a neuroprotective role in NGF-withdrawn neurons at the early stage of programmed cell death, but accumulated APP promotes apoptosis of compromised DRG neurons under continued NGF-absent conditions. Thus, we infer that APP increases to protect neurons from neurodegenerative insults but induces apoptosis when the insults persist.

XV. APP induces neuronal apoptosis via internal disintegration

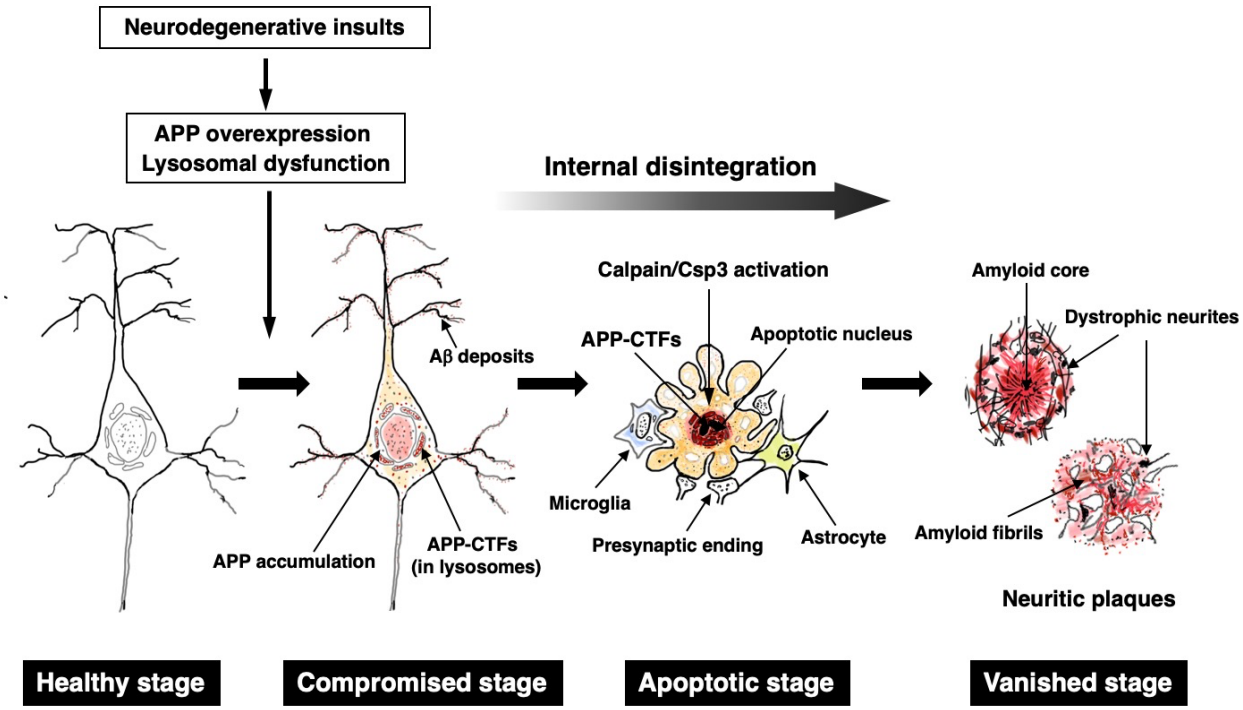

Figure 15. APP induces neuronal apoptosis via internal disintegration. Hypothetical explanation for APP-induced internal disintegration of pyramidal neurons in AD. The diagram at the apoptotic stage is based on the experimental data shown in Figs. 8-11 and 13 and combined with the scheme shown in Fig.7. See text for details.

The process of neuronal internal disintegration focused on APP-induced apoptosis is schematized in Fig. 15. APP expression is rapidly elevated during the early period of neuronal differentiation in P19 EC cells (Yoshikawa et al., 1990) and NGF-treated DRG sensory neurons (Nishimura et al., 2003), suggesting that APP promotes neuronal differentiation and vitality ("Healthy stage"). Neuroprotective effects of wild-type APP have also been reported from other laboratories (Perez et al., 1997; Xu et al., 1999). Neurodegenerative insults (e.g., traumatic brain injury, oxidative damage, hypoxia, distress, aging) induce overexpression of APP, which initially protects neurons from degeneration, and lysosomal dysfunction propels the accumulation of APP. At this stage, Aβ is deposited around compromised neurons ("Compromised stage"). When APP accumulation in the lysosomes reaches a critical level, the calpain-Csp3 pathway is activated to induce apoptotic changes such as nuclear fragmentation and cytoplasmic membrane blebbing (see Figs. 8 and 9) ("Apoptotic stage"). Amyloidogenic APP-CTFs form primordial amyloid fibrils near the nucleus (see Fig. 4). APP-CTFs are also present inside the nucleus (see Fig. 13). After degenerated neurons are completely scavenged by astrocytes and microglial cells, amyloid fibrils and dystrophic neurites, which are resistant to the glial clearance, remain as neuritic plaques at the extracellular space ("Vanished stage").

Similar ideas to the internal disintegration hypothesis have been reported from other laboratories studying mutant APP transgenic mice. In transgenic AD model mice carrying mutated APP/Tau/presenilin genes, an amyloid conformation-dependent monoclonal antibody reacts with perinuclear and later nuclear compartments immunoreactive for Aβ and APP-CTFs in compromised neurons, implying that intraneuronal amyloid accumulation results in extracellular neuritic plaques after neuronal death (Pensalfini et al., 2014). Mutant human APP-transgenic mice exhibit declines in autolysosome acidification in neurons where Aβ/APP-CTFs are accumulated within enlarged autolysosomes well before extracellular amyloid deposition appears (Lee et al., 2022). In these compromised neurons, abundant Aβ-immunoreactive autophagic vacuoles pack into large membrane blebs, exhibiting unique flower-like perikaryal rosettes, which are also observed in AD brains. Noteworthily, neurons at the apoptotic stage during internal disintegration closely resemble those seen in these transgenic mice.

XVI. Evidence corroborating the internal disintegration hypothesis

Several studies have shown a close link between APP and neuronal apoptosis associated with cysteine proteases including caspases and calpains in developmental programmed cell death and AD. APP expression increases in dying motoneurons where APP serves as a substrate of activated Csp3 (Barnes et al., 1998). Csp3 increases in dying hippocampal neurons of AD brains, and its cleaved APP product colocalizes with Aβ in APs (Gervais et al., 1999). Both activated Csp3 and cleaved APP products in the hippocampal and frontal cortex are increased in AD (Zhao et al., 2003). Calpains have also been implicated in the neurodegeneration of AD. Calpain is significantly activated in the prefrontal cortex from patients with AD but not from those with Huntington's disease, indicating AD-specific activation of calpain (Saito et al., 1993). A marked depletion of calpastatin, an endogenous calpain inhibitor, mediated by activated cysteine proteases promotes neurodegeneration in AD (Rao et al., 2008).

Lysosomal dysfunctions are most likely to contribute to APP-induced neurodegeneration in AD. Presenilin, a core component of the γ-secretase complex that cleaves APP (see Fig. 2), is involved in the maintenance of lysosomal function by ensuring proper lysosome acidification.

Presenilin plays a crucial role in maintaining lysosomal Ca^{2+} homeostasis via lysosomal acidification, which is essential for proper autophagy and proteolysis (Nixon et al., 2008). Hippocampal neurons in transgenic mice carrying mutant presenilin are hypersensitive to DNA damage that correlates with increased intracellular Ca^{2+} levels, calpain activation, and neuronal apoptosis (Chan et al., 2002). Neurons in aging mice carrying mutated presenilin/APP transgenes exhibit apoptotic changes such as DNA fragmentation and Csp3 activation (Yang et al., 2008). Of note, transgenic AD model mice that exhibit intraneuronal accumulations of Aβ and APP-CTFs also carry mutated presenilin genes (Pensalfini et al., 2014; Lee et al., 2022). Nixon (2024) discusses that a lack of balance between enhanced autophagy induction and diminished lysosomal function in vulnerable pyramidal neuron populations leads to intracellular accumulations of Aβ and APP-CTFs in plaque-like aggregates that become extracellular senile plaques after neuronal disappearance, emphasizing the link between autophagy-associated lysosomal dysfunction and APP-induced neuropathology in AD.

Densities of pyramidal neurons in the neocortex and hippocampus correlate with those of neuritic plaques (see Fig. 1B). These pyramidal neurons express a large amount of APP for maintaining their complex functions and require high lysosomal activities to metabolize it. The number and size of pyramidal neurons in the association cortices of mammalian brains increased over evolutionary time to reach the highest figures in the human brain. Thus, it is speculated that these neurons emerged at the final stage of mammalian brain evolution greatly heightened cognitive functions of humans but simultaneously became highly vulnerable to APP-induced degeneration. The internal disintegration of pyramidal neurons in AD is reminiscent of “cosmic supernova” in which a massive star undergoes internal disintegration at the end of its life, resulting in an explosion that discharges its ingredients into space and leaves “supernova remnants” behind.

Acknowledgements

The author expresses gratitude to Drs. Tsuyoshi Ishii (for support and research materials), Kei Maruyama, Yokichi Hayashi, and Takako Aizawa (for collaborations from 1986 to 1992) at the Psychiatric Research Institute of Tokyo, and to Drs. Isao Nishimura, Taichi Uetsuki, and Ken-ichiro Kuwako (for collaborations from 1994 to 2003) at the Institute for Protein Research, The University of Osaka.

References

Andrews PW (1984) Retinoic acid induces neuronal differentiation of a cloned human embryonal carcinoma cell line in vitro. Dev Biol 103:285–293.

Arnold SE, Hyman BT, Flory J, Damasio AR, Van Hoesen GW (1991) The topographical and neuroanatomical distribution of neurofibrillary tangles and neuritic plaques in the cerebral cortex of patients with Alzheimer's disease. Cereb Cortex 1:103–116.

Barnes NY, Li L, Yoshikawa K, Schwartz LM, Oppenheim RW, Milligan CE (1998) Increased production of amyloid precursor protein provides a substrate for caspase-3 in dying motoneurons. J Neurosci 18:5869–5880.

Benowitz LI, Rodriguez W, Paskevich P, Mufson EJ, Schenk D, Neve RL (1989) The amyloid precursor protein is concentrated in neuronal lysosomes in normal and Alzheimer disease subjects. Exp Neurol 106:237–250.

Braak H, Braak E, Kalus P (1989) Alzheimer's disease: areal and laminar pathology in the occipital isocortex. Acta Neuropathol 77:494–506.

Chan SL, Culmsee C, Haughey N, Klapper W, Mattson MP (2002) Presenilin-1 mutations sensitize neurons to DNA damage-induced death by a mechanism involving perturbed calcium homeostasis and activation of calpains and caspase-12. Neurobiol Dis 11:2–19.

Dyrks T, Weidemann A, Multhaup G, Salbaum JM, Lemaire HG, Kang J, Müller-Hill B, Masters CL, Beyreuther K (1988) Identification, transmembrane orientation and biogenesis of the amyloid A4 precursor of Alzheimer's disease. EMBO J 7:949–957.

Gervais FG, Xu D, Robertson GS, Vaillancourt JP, Zhu Y, Huang JQ, LeBlanc A, Smith D, Rigby M, Shearman MS, Clarke EE, Zheng H, Van Der Ploeg LHT, Ruffolo SC, Thornberry NA, Xanthoudakis S, Zamboni RJ, Roy S, Nicholson DW (1999) Involvement of caspases in proteolytic cleavage of Alzheimer's amyloid-β precursor protein and amyloidogenic Aβ peptide formation. Cell 97:395–406.

Glenner GG, Wong CW (1984) Alzheimer's disease: Initial report of the purification and characterization of a novel cerebrovascular amyloid protein. Biochem Biophys Res Commun 120:885–890.

Hardy J, Higgins G (1992) Alzheimer's disease : The amyloid cascade hypothesis. Science 256: 184–185.

Hayashi Y, Kashiwagi K, Yoshikawa K (1992) Protease inhibitors generate cytotoxic fragments from Alzheimer amyloid protein precursor in cDNA-transfected glioma cells. Biochem Biophys Res Commun 187:1249–1255.

Kametani F, Haga S, Tanaka K, Ishii T (1990) Amyloid β-protein precursor (APP) of cultured cells: Secretory and non-secretory forms of APP. J Neurol Sci 97:43–52.

Kang J, Lemaire HG, Unterbeck A, Salbaum JM, Masters CL, Grzeschik KH, Multhaup G, Beyreuther K, Müller-Hill B (1987) The precursor of Alzheimer's disease amyloid A4 protein resembles a cell-surface receptor. Nature 325:733–736.

Kuwako KI, Nishimura I, Uetsuki T, Saido TC, Yoshikawa K (2002) Activation of calpain in cultured neurons overexpressing Alzheimer amyloid precursor protein. Mol Brain Res 107:166–175.

Lee JH, Yang DS, Goulbourne CN, Im E, Stavrides P, Pensalfini A, Chan H, Bouchet-Marquis C, Bleiwas C, Berg MJ, Huo C, Peddy J, Pawlik M, Levy E, Rao M, Staufenbiel M, Nixon RA (2022) Faulty autolysosome acidification in Alzheimer's disease mouse models induces autophagic build-up of Aβ in neurons, yielding senile plaques. Nat Neurosci 25:688–701.

Lu DC, Rabizadeh S, Chandra S, Shayya RF, Ellerby LM, Ye X, Salvesen GS, Koo EH, Bredesen DE (2000) A second cytotoxic proteolytic peptide derived from amyloid β-protein precursor. Nat Med 6:397–404.

Maruyama K, Terakado K, Usami M, Yoshikawa K (1990) Formation of amyloid-like fibrils in COS cells overexpressing part of the Alzheimer amyloid protein precursor. Nature 347:566–569.

McBurney MW, Jones-Villeneuve EM V., Edwards MKS, Anderson PJ (1982) Control of muscle and neuronal differentiation in a cultured embryonal carcinoma cell line. Nature 299:165–167.

Nishimura I, Takazaki R, Kuwako KI, Enokido Y, Yoshikawa K (2003) Upregulation and antiapoptotic role of endogenous Alzheimer amyloid precursor protein in dorsal root ganglion neurons. Exp Cell Res 286:241–251.

Nishimura I, Uetsuki T, Dani SU, Ohsawa Y, Saito I, Okamura H, Uchiyama Y, Yoshikawa K (1998) Degeneration in vivo of rat hippocampal neurons by wild-type Alzheimer amyloid precursor protein overexpressed by adenovirus-mediated gene transfer. J Neurosci 18:2387–2398.

Nishimura I, Uetsuki T, Kuwako K, Hara T, Kawakami T, Aimoto S, Yoshikawa K (2002) Cell death induced by a caspase-cleaved transmembrane fragment of the Alzheimer amyloid precursor protein. Cell Death Differ 9:199–208.

Nixon RA (2024) Autophagy–lysosomal-associated neuronal death in neurodegenerative disease. Acta Neuropathol 148:42 Available at: https://doi.org/10.1007/s00401-024-02799-7.

Nixon RA, Yang DS, Lee JH (2008) Neurodegenerative lysosomal disorders: A continuum from development to late age. Autophagy 4:590–599.

Pensalfini A, Albay R, Rasool S, Wu JW, Hatami A, Arai H, Margol L, Milton S, Poon WW, Corrada MM, Kawas CH, Glabe CG (2014) Intracellular amyloid and the neuronal origin of Alzheimer neuritic plaques. Neurobiol Dis 71:53–61.

Perez RG, Zheng H, Van Der Ploeg LHT, Koo EH (1997) The β-amyloid precursor protein of Alzheimer's disease enhances neuron viability and modulates neuronal polarity. J Neurosci 17:9407–9414.

Rao M V., Mohan PS, Peterhoff CM, Yang DS, Schmidt SD, Stavrides PH, Campbell J, Chen Y, Jiang Y, Paskevich PA, Cataldo AM, Haroutunian V, Nixon RA (2008) Marked calpastatin (CAST) depletion in Alzheimer's disease accelerates cytoskeleton disruption and neurodegeneration: Neuroprotection by CAST overexpression. J Neurosci 28:12241–12254.

Rohn TT, Ivins KJ, Bahr BA, Cotman CW, Cribbs DH (2000) A monoclonal antibody to amyloid precursor protein induces neuronal apoptosis. J Neurochem 74:2331–2342.

Saito KI, Elce JS, Hamos JE, Nixon RA (1993) Widespread activation of calcium-activated neutral proteinase (calpain) in the brain in Alzheimer disease: A potential molecular basis for neuronal degeneration. Proc Natl Acad Sci U S A 90:2628–2632.

Tominaga K, Uetsuki T, Ogura A, Yoshikawa K (1997) Glutamate responsiveness enhanced in neurones expressing amyloid precursor protein. Neuroreport 8:2067–2072.

Uetsuki T, Takemoto K, Nishimura I, Okamoto M, Niinobe M, Momoi T, Miura M, Yoshikawa K (1999) Activation of neuronal caspase-3 by intracellular accumulation of wild- type Alzheimer amyloid precursor protein. J Neurosci 19:6955–6964.

Xu X, Yang D, Wyss-Coray T, Yan J, Gan L, Sun Y, Mucke L (1999) Wild-type but not Alzheimer-mutant amyloid precursor protein confers resistance against p53-mediated apoptosis. Proc Natl Acad Sci U S A 96:7547–7552.

Yang DS, Kumar A, Stavrides P, Peterson J, Peterhoff CM, Pawlik M, Levy E, Cataldo AM, Nixon RA (2008) Neuronal apoptosis and autophagy cross talk in aging PS/APP mice, a model of Alzheimer's disease. Am J Pathol 173:665–681

Yoshikawa K (1993) Neurotoxicity of β-amyloid (scientific correspondence). Nature 361:122–123.

Yoshikawa K (1995) Neurotoxicity of amyloid β-protein and the amyloid β-protein precursor. In: Pathobiology of Alzheimer's Disease (Goate A, Ashall F, eds), pp 145–165. London: Academic Press.

Yoshikawa K, Aizawa T, Hayashi Y (1992) Degeneration in vitro of post-mitotic neurons overexpressing the Alzheimer amyloid protein precursor. Nature 359:64–67.

Yoshikawa K, Aizawa T, Maruyama K (1990) Neural differentiation increases expression of Alzheimer amyloid protein precursor gene in murine embryonal carcinoma cells. Biochem Biophys Res Commun 171:204–209.

Yoshikawa K, Maruyama K, Terakado K, Usami M, Aizawa T (1991) A DNA-transfected cell model for Alzheimer amyloidogenesis: Demonstration of primordial amyloid fibrils in COS cells. In: Frontiers of Alzheimer Research (Ishii T, Allsop D, Selkoe DJ, eds), pp 217-227 Amsterdam: Elsevier Science Publishers B.V.

Zhao M, Su J, Head E, Cotman CW (2003) Accumulation of caspase cleaved amyloid precursor protein represents an early neurodegenerative event in aging and in Alzheimer's disease. Neurobiol Dis 14:391–403.